

Article

Field Complete Coverage Path Planning Based on Improved Genetic Algorithm for Transplanting Robot

Xizhi Wu ^{1,†} , Jinqiang Bai ^{1,†}, Fengqi Hao ^{1,*}, Guanghe Cheng ¹, Yongwei Tang ² and Xiuhua Li ¹

¹ Shandong Provincial Key Laboratory of Computer Networks, Shandong Computer Science Center (National Supercomputer Center in Jinan), QiLu University of Technology (Shandong Academy of Sciences), 19 Keyuan Road, Jinan 250014, China

² Key Laboratory of High Efficiency and Clean Mechanical Manufacture, School of Mechanical Engineering, Ministry of Education, Shandong University, 17923 Jingshi Road, Jinan 250061, China

* Correspondence: haofq@sdas.org

† These authors contributed equally to this work.

Abstract: The Complete Coverage Path Planning (CCPP) is a key technology in the field of agricultural robots, and has great significance for improving the efficiency and quality of tillage, fertilization, harvesting, and other agricultural robot operations, as well as reducing the operation energy consumption. The traditional boustrophedon- or heuristic-search-algorithm-based CCPP methods, when coping with the field with irregular boundaries, obstacles, and other complex environments, still face many problems and challenges, such as large repeated work areas, multiple turns or U-turns, low operation efficiency, and prone to local optimum. In order to solve the above problems, an improved-genetic-algorithm-based CCPP method was proposed in this paper, the proposed method innovatively extends the traditional genetic algorithm's chromosomes and single-point mutation into chromosome pairs and multi-point mutation, and proposed a multi-objective equilibrium fitness function. The simulation and experimental results on simple regular fields showed that the proposed improved-genetic-algorithm-based CCPP method achieved the comparable performance with the traditional boustrophedon-based CCPP method. However, on the complex irregular fields, the proposed CCPP method reduces 38.54% of repeated operation area and 35.00% of number of U-turns, and can save 7.82% of energy consumption on average. This proved that the proposed CCPP method has a strong adaptive capacity to the environment, and has practical application value in improving the efficiency and quality of agricultural machinery operations, and reducing the energy consumption.

Keywords: complete coverage path planning; genetic algorithms; autonomous agricultural robot; field efficiency



Citation: Wu, X.; Bai, J.; Hao, F.; Cheng, G.; Tang, Y.; Li, X. Field Complete Coverage Path Planning Based on Improved Genetic Algorithm for Transplanting Robot. *Machines* **2023**, *11*, 659. <https://doi.org/10.3390/machines11060659>

Academic Editor: Augusto Luis Ballardini

Received: 17 May 2023
Revised: 13 June 2023
Accepted: 14 June 2023
Published: 19 June 2023



Copyright: © 2023 by the authors. Licensee MDPI, Basel, Switzerland. This article is an open access article distributed under the terms and conditions of the Creative Commons Attribution (CC BY) license (<https://creativecommons.org/licenses/by/4.0/>).

1. Introduction

The traditional agricultural robot operations relying on manual control have low operation efficiency, high energy consumption, poor safety, and the quality of operation depends on the experience of agricultural machinery operators [1]. Moreover, due to the increasing shortage of rural labor force, they are unable to meet the requirements of modern agricultural development. Therefore, the automatic driving technology has become the research focus in the intelligent planters, transplanters, harvesters, and other intelligent agricultural robots [2–5]. The farmland Complete Coverage Path Planning (CCPP), as one of the key technologies in autonomous agricultural robots [6], aims at finding paths that cover all operating areas except obstacles. It has great significance for improving the operation efficiency of automatic driving agricultural robot, reducing the repeated work area and energy consumption [7], ensuring the operation quality [8], and promoting the development of precision agriculture [9].

The CCPP methods mainly address the following problems [10–12], (1) the entire work area must be traversed; (2) the static obstacles must be avoided; (3) the repeated work areas

should be reduced as much as possible; and (4) the number of turns and U-turns should be minimized. The CCPP methods can be classified as grid-based method, cell decomposition-based method, neural network-based method, and heuristic algorithm-based method according to its implementation method.

The grid-based method, invented by W.E. Howden in 1968, divides the work area into several grids with equal size, and seeks the optimal path that has the minimum number of repeated grids and traverses all free grids. A high-resolution grid map representation-based online CCPP control algorithm [13] was proposed to generate a smooth coverage path through Bezier curve approximation. The grid and HS (Harmony Search) algorithm-based path planner [14] significantly reduced the number of trajectories turns. To solve the problem of path planning with a large number of grids, Ammar et al. [15] improved the calculation times of the actual cost function. The grid-based methods have the advantages of simple implementation and easy planning; however, their computational complexity increases with the increasing number of grids.

The cell decomposition-based method firstly decomposes the work area into multiple sub-regions with simple shapes and without obstacles. Then the CCPP of each sub-region becomes a simple reciprocating movement, and can be implemented by seeking the optimal operation sequence of each sub-region. The boustrophedon-based decomposition method [16] was presented to divide the region with excessive obstacle vertices. The decomposition method [17] using different decomposition directions for different farmlands solved the problem that the traditional method can only be decomposed vertically. Although the cell decomposition methods have high efficiencies and significantly reduced the CCPP difficulty, the inappropriate connecting order of each sub-region can result in too many repeated paths.

The neural network-based CCPP method utilizes the self-learning ability and adaptability of neural network to improve the area coverage efficiency. A biologically inspired neural networks-based CCPP method [18] was emerged to plan collision-free paths autonomously and in real time. The neural dynamics-based complete coverage navigation (CCN) algorithm [19] can plan a shorter collision-free complete coverage path in an unknown environment. A complete coverage neural network (CCNN) [20] was constructed, which can generate paths with smaller steering angles and fewer changes in navigation direction by the next optimal location decision strategy that combined with the driving direction. A feature-learning fully convolutional model [21] was built to solve the crop row-based CCPP problem. The neural network brings new ideas to solve the CCPP problem, whereas it has a lower planning success rate when the data are insufficient, and its loss function has less robustness.

The heuristic algorithms-based CCPP method utilizes the heuristic factors to reduce the complexity of the search problem, thereby improving the efficiency of searching the optimal paths. The bacterial foraging method [22] for robot path planning is proposed to plan the best collision-free path between the starting point and the target point, and it can plan stable and reliable trajectories in complex environments. A new mix-opt operator for simulated annealing algorithm [23] was proposed to accelerate the convergence speed of heuristic optimization. The CCPP method combining the genetic algorithm and TSP (Travel Quotient Problem) [24] can find the coverage path that has the shortest travel distance and grid coverage time. A novel integrated virus evolution heuristic algorithm [25] that satisfies the trade-off between multiple objectives is proposed for intelligent toolpath optimization, which can obtain the direct output of the global optimized toolpath, and has very important industrial strategic capabilities. The Non-Dominated Sorting Genetic Algorithm (NSGA-III) [26] takes the maximum volume of pesticide tanks into consideration, and can seek out the coverage path with minimum travel distance and routing angle. It can solve the CCPP problem of multi-agricultural mobile robot. A self-reconfigurable autonomous robot [27] that can enter the narrow space was created, and can conduct the CCPP by optimizing the order of traveler sequences. Focusing on the irregular fields with a single entrance, a search space with virtual obstacles [28] was generated that can use the A* algorithm to

determine a curved path for returning to the entrance after completed an agricultural task. The heuristic algorithm-based CCPP methods have the advantages of easy implementation, high capability of seeking the optimum solution, and fair extensibility [29].

Many scholars have done in-depth research on complete coverage path planning technology, which is of significance for the further research and application of this technology in intelligent agricultural robots. Each path planning method mentioned above has its own advantages and limitations, and their differences are summarized in Table 1, a comparison table of complete coverage path planning methods. Among them, the genetic algorithm has the advantages of high optimization ability and parallel ability, easy coding, and combination with other algorithms, and can effectively solve multi-objective optimization problems. Hence, this paper uses the improved genetic algorithm to solve the complete coverage path planning problem.

Table 1. Comparison table of complete coverage path planning methods.

| Algorithm | Descriptions |
|---------------------------|--|
| Grid method | Simple implementation and convenient planning The complexity increases with the increase in the grid |
| Cell decomposition method | Convenient and fast, reducing the difficulty of CCPP Unreasonable connection order lead to repeated paths |
| Neural network method | Excellent real-time and obstacle avoidance The robustness of the error function is poor |
| Heuristic algorithm | Strong optimization ability and scalability Unstable performance, easy to fall into local optimum |

The grid-based, cell decomposition-based, and neural network-based CCPP methods have obtained many research achievements; however, they still have some problems such as high path repetition rate, low planning efficiency, and poor robustness when coping with complex working scenarios. Therefore, the heuristic-based CCPP method with good stability and strong global optimization-seeking ability was used in this paper to deal with the complex farming scenarios that have irregular boundaries and obstacles. Nonetheless, the adopted classical heuristic genetic algorithm is prone to the local optimal solution in the actual planning. Thus, an improved genetic algorithm-based [30] CCPP method was proposed in this paper to improve the global optimization-seeking ability and environmental adaptability of the classical genetic algorithm in complex environments. The proposed method innovatively extends the traditional genetic algorithm's chromosomes and single-point mutation into chromosome pairs and multi-point mutation, which can reduce the repeated area and the number of turns and U-turns. The proposed CCPP method can guide the autonomous agricultural robot to achieve efficient cultivation especially in complex field environments. The main contributions of this paper are as follows, (1) extends the chromosomes to chromosome pairs that contains a chromosome for genetic evolution and a chromosome for fitness calculation, which increases the efficiency and operational effectiveness of CCPP; (2) proposes a multi-point mutation method to break the genetic sequence of the parent chromosomes as much as possible, which improves the global optimization-seeking ability in a complex environment; and (3) establishes a multi-objective fitness function that takes account of the repeated operation area, the number of turns and U-turns, which reduces the overall energy consumption.

2. Materials and Methods

The proposed improved-genetic-algorithm-based CCPP method consists of two parts, (1) the field environment map modeling and (2) the improved genetic algorithm for CCPP. As shown in Figure 1, the field environment map modeling includes three modules, (1) environment map rasterization, which divides the environment map into grids with equal size; (2) irregular object dilation, which dilates the irregular-sized obstacles and

irregular-shaped fields into regular grids; and (3) grid map coding, which adopts the sequential notation method to code the grids. The improved genetic algorithm for CCPP includes six modules, (1) chromosome-pairs-based initial population generation, which generates the initial Q chromosome pairs; (2) multi-objective-balance-criterion-based chromosome fitness calculation, which is used for algorithm iterative update; (3) elitist-strategy-based roulette selection, which selects a limited number of chromosomes with the best fitness values to pass to the next generation population; (4) order-preserving crossover, which aims to inherit the excellent genes of the parent chromosomes and ensure the stability of the population; (5) multi-points mutation, which introduces diversity in the genetic population and expands the search space; and (6) optimal complete coverage path (OCCP) output, which decodes and outputs the OCCP when the termination condition is satisfied.

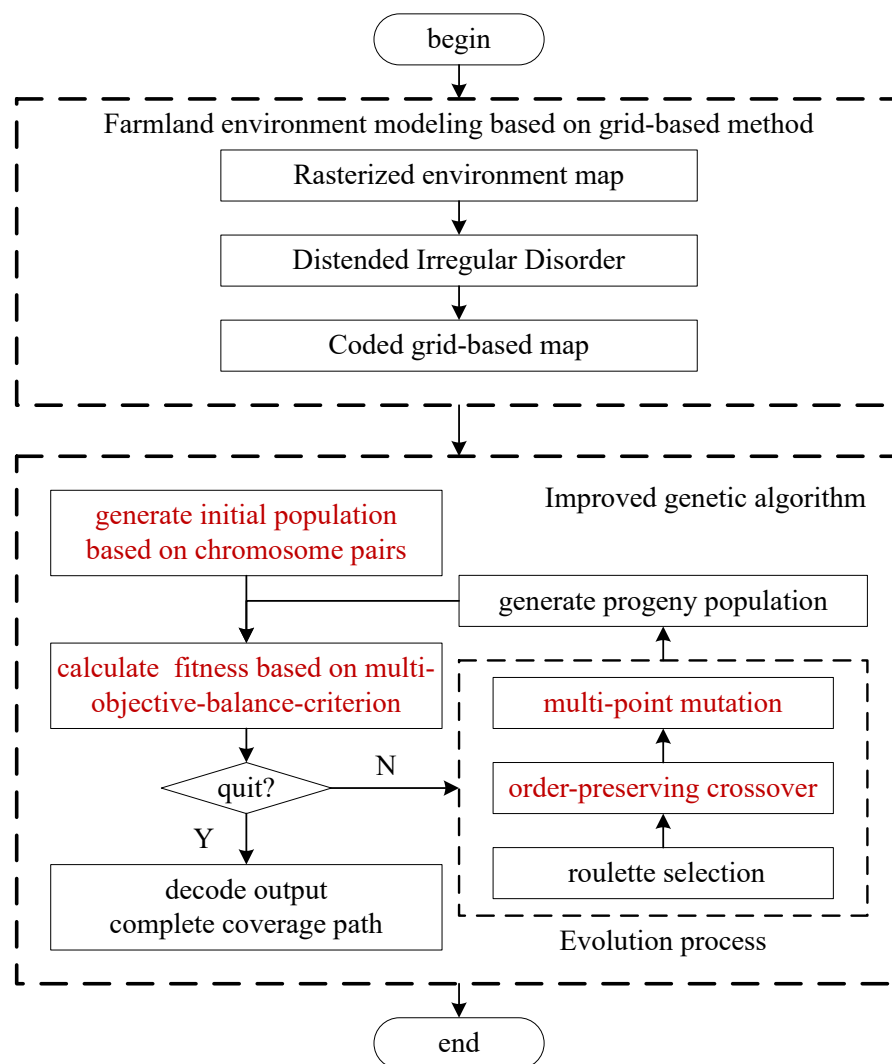


Figure 1. Flow chart of CCPP method based on improved genetic algorithm.

2.1. Field Environment Map Modeling Based on Grid Method

The field environment mapping is the foundation of CCPP for self-driving agricultural robots. The grid map can accurately represent the environmental information, and is easy to maintain, store, and be used for solving the CCPP problem. Therefore, the grid map construction method was adopted in this paper for representing the field boundaries, free space, and obstacles in a real field. The grid-map-based field environment modeling includes (1) environment map rasterization, (2) irregular object dilation, and (3) grid map coding, which are detailed as follows.

2.1.1. Rasterization of the Environment Map

The environment map rasterization is the first task for creating the environment grid map, which divides the environment map into grids with equal area. As shown in Figure 2, the field map shown in Figure 2a is rasterized into the grid map shown in Figure 2b. The grid size can be determined by the size and the operation width of the autonomous driving agricultural robot. In addition, the obstacles are projected to the grid map, e.g., the obstacle A and B in Figure 2.

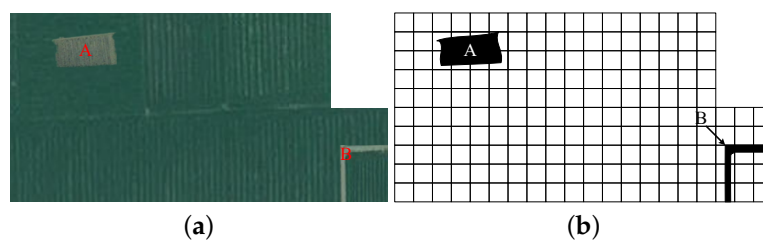


Figure 2. Field environment map rasterization. (a) The actual field area. (b) The grid-based map.

2.1.2. Irregular Grid Expansion

When the field has an irregular shape or some static obstacles existed in the field, the rasterized field map needs to be dilated into a regular-shaped map, and the irregular-shaped obstacles into regular-shaped obstacles. This will help to determine whether a grid is reachable. For example, the grid map shown in Figure 2b was dilated to the grid map shown in Figure 3. Area C in Figure 3 was added to regularize the grid map and the irregular-shaped obstacle A in Figure 2b were dilated into the regular-shaped obstacle A' in Figure 3. In addition, because the area D in Figure 3 surrounded by L-shaped obstacle B in Figure 2b is an unreachable, the L-shaped obstacle B in Figure 2b should be dilated into the rectangular obstacle B' in Figure 3.

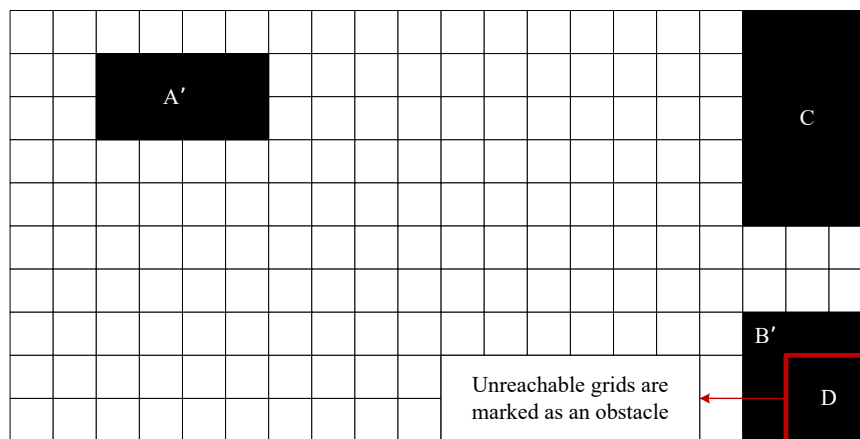


Figure 3. The grid-based map after irregular grid expansion

2.1.3. Grid-Based Map Coding

For the convenience of solving the CCP problem and presenting the final planned path, the sequential notation method was adopted to encode the map grids in this paper. As shown in Figure 4, the grid map was encoded, starting from the bottom left grid, and each grid is sequentially marked as the unique number in the order of left to right and bottom to top. Meanwhile, the black occupied grid (e.g., 18–20, 143–146, 118–120) was labeled as “1”, and the white free grid (e.g., 61–117) as “0”, for identifying the properties of different grids. Therefore, each grid is represented as $\langle ID, Prop \rangle$, where $ID \in \mathbb{N}$ is the unique number of the grid, and $Prop \in \{0, 1\}$ is the grid property. When the CCP method searches for the OCPP, the 4-neighbor searching method was employed for reducing the

CCPP searching spaces. For example, if the autonomous driving agricultural robot is at the position $\langle 90,0 \rangle$ in Figure 4, its 4-neighbor were $\langle 89,0 \rangle$, $\langle 91,0 \rangle$, $\langle 70,0 \rangle$, and $\langle 110,0 \rangle$, namely the one-step reachable search domain of the grid $\langle 90,0 \rangle$. For ease of calculating the number of turns and U-turns (see Section 2.2.2), the left movement (e.g., from $\langle 90,0 \rangle$ to $\langle 89,0 \rangle$ in Figure 4 is marked as 1, up movement (e.g., from $\langle 90,0 \rangle$ to $\langle 110,0 \rangle$ in Figure 4 as 2, right movement (e.g., from $\langle 90,0 \rangle$ to $\langle 91,0 \rangle$ in Figure 4 as 3 and down movement (e.g., from $\langle 90,0 \rangle$ to $\langle 70,0 \rangle$ in Figure 4 as 4.

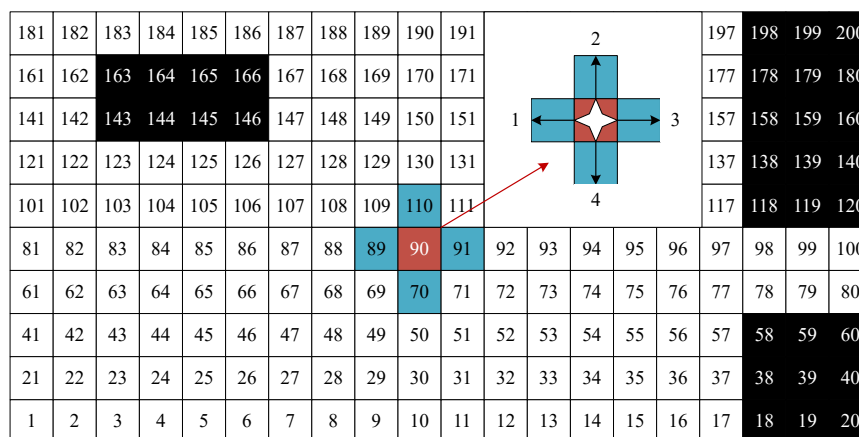


Figure 4. Grid-based map encoding.

2.2. Field CCPP Based on Improved Genetic Algorithm

Since the traditional-genetic-algorithm-based CCPP method, when coping with the irregular-shaped field, and other complex field with obstacles, is prone to the problems, such as more repeated work area, more turns or U-turns, and falling into local optimum, an improved-genetic-algorithm-based CCPP method was proposed in this paper. This method innovatively proposes the chromosome pairs and multi-points mutation to improve its global optimization ability in complex environments, and the multi-objective (i.e., the repeated work area, the number of turns and U-turns)-balance-criterion-based chromosome fitness function to reduce the number of turns and U-turns under the premise of less repeated work area. The improved genetic algorithm includes (1) chromosome-pair-based initial population generation, (2) multi-objective-balance-criterion-based chromosome fitness calculation, (3) elitist-strategy-based roulette selection, (4) order-preserving crossover, (5) multi-points mutation, and (6) OCCP output, which are detailed as follows. Furthermore, the algorithm needs to meet the following conditions, (1) the shape of the grid map is a regular rectangle; (2) the number of grids in the grid map is limited; (3) the feasible area and obstacle area of the known grid map; and (4) does not consider the mileage constraints of agricultural robots. At the end of the algorithm run, the output optimal chromosome is decoded into the optimal path order.

2.2.1. Initial Population Generation Based on Chromosome Pairs

The CCPP aims to traverse all the free grids, and the traversed grid order is the planned complete coverage path. To describe the encoding scheme with a minimum encoding character set, a decimal encoding is adopted in this paper. Each chromosome represents a feasible solution, i.e., a field complete coverage path, where the grid in set S_w presents at least once, while the grid in set S_o is absent. For example, an initial chromosome X_{ch} in Figure 5b corresponding to the encoded grid map in Figure 5a, can be randomly generated.

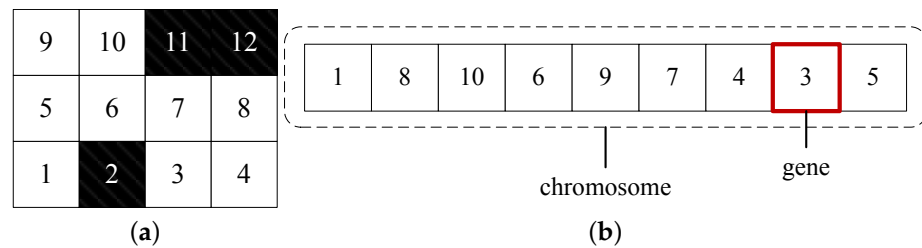


Figure 5. The initial chromosome. (a) Coded map (b) Generated chromosome randomly.

The traditional genetic algorithm randomly generates Q chromosomes as the initial population. However, for the CCP problem, the randomly generated initial population is prone to a large number of invalid chromosomes. For example, the chromosome shown in Figure 5b is an invalid chromosome since the 4-neighbor relationship between gene 1 and gene 8 is not satisfied, i.e., gene 8 is not in the one-step reachable search domain of gene 1. In other words, the autonomous driving agricultural robot cannot directly move from grid 1 to grid 8. Therefore, the randomly generated chromosome is adjusted in this paper to obtain the chromosome (as shown in Figure 6) that the adjacent genes satisfied the 4-neighbor relationship.

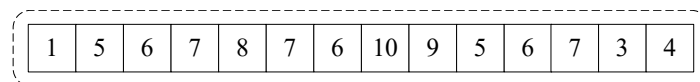


Figure 6. The adjusted chromosome.

The proposed adjustment method of the chromosome is described as follows:

- (1) If two adjacent genes satisfy the 4-neighbor relationship, i.e., the adjacent genes are one-step reachable, no adjustment is required.
- (2) If two adjacent genes do not satisfy the 4-neighbor relationship, the gene sequence where the adjacent genes satisfy the 4-neighbor relationship with the shortest path was inserted between the two genes. If the inserted gene appears in the subsequent gene sequence of the chromosome, the repeated genes appeared in the subsequent gene sequence will be deleted. The Floyd's algorithm [31] was used in this paper to find the gene sequence with the shortest path that should be inserted.
- (3) Starting from the first gene of the chromosome, step (1) and step (2) were repeated until all the genes of the chromosome were traversed. Thus, the valid chromosome where all the adjacent genes satisfy the 4-neighbor relationship will be generated.

For example, the process of adjusting the invalid chromosome shown in Figure 5b to the valid chromosome shown in Figure 6 is as follows:

- (1) As shown in Figure 7a, starting from the first gene, the shortest path 5-6-7 obtained by the Floyd's algorithm was inserted between gene 1 and gene 8 since gene 1 and gene 8 do not satisfy the 4-neighbor relationship. In addition, the genes 5, 6, and 7 appeared in the subsequent gene sequence of the chromosome are deleted, and the adjusted chromosome 1-5-6-7-8-10-9-4-3 will be obtained.
- (2) As shown in Figure 7b, next traversing the gene 8, the shortest path 7-6 obtained by the Floyd's algorithm was inserted between gene 8 and gene 10 since gene 8 and gene 10 do not satisfy the 4-neighbor relationship. Because gene 7 and gene 6 was absent in the subsequent gene sequence, the chromosome 1-5-6-7-8-7-6-10-9-4-3 can be obtained without gene deletion operation.
- (3) As shown in Figure 7c, continually traversing the next gene 10, because gene 10 and gene 9 satisfy the 4-neighbor relationship, no adjustment was done. Then traversing the next gene 9, as shown in Figure 7d, the shortest path 5-6-7-3 was inserted similarly as (1) between gene 9 and gene 4, and the repeated gene 3 was deleted. Since gene 4 was the last gene of the chromosome, the chromosome adjustment was

finished. Finally, the adjusted valid chromosome is 1-5-6-7-8-7-6-10-9-5-6-7-3-4 where all free grids appeared at least once and all the adjacent genes satisfy the 4-neighbor relationship.

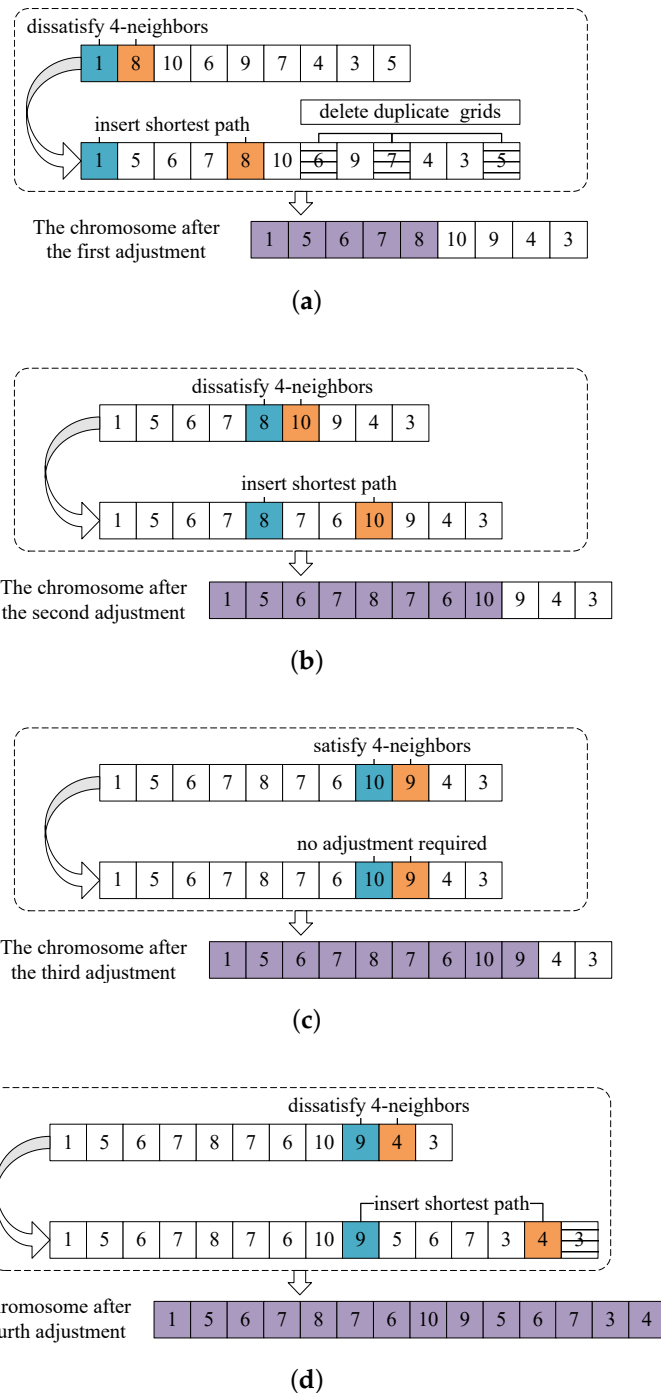


Figure 7. The initial chromosome adjustment. (a) Need to adjust two not adjacent genes. (b) Insert the shortest path. (c) No need to adjust two adjacent genes. (d) Adjustment to the end of the last gene position.

As shown in Figure 7, the chromosome pair was generated by combining the chromosome $X_{ch} = 1-8-10-6-9-7-4-3-5$ and the adjusted valid chromosome $Y_{ch} = 1-5-6-7-8-7-6-10-9-5-6-7-3-4$. Thus, the initial population $P_{init} = \{ \langle X_1|Y_1 \rangle, \langle X_2|Y_2 \rangle, \dots, \langle X_Q|Y_Q \rangle \}$ show in Figure 8 can be obtained by combing the Q chromosomes $\{X_1, X_2, \dots, X_Q\}$ randomly generated by the traditional genetic algorithm and its adjusted valid chromosomes

$\{Y_1, Y_2, \dots, Y_Q\}$. The chromosome X in the initial population has the same number of genes, and was used for selection, crossover, mutation, and other evolutionary operations. The chromosome Y in the initial population may have different number of genes, and was used for chromosome fitness calculation. Moreover, the chromosome Y represents a complete coverage path that an autonomous driving agricultural robot can travel in the real farming operation.

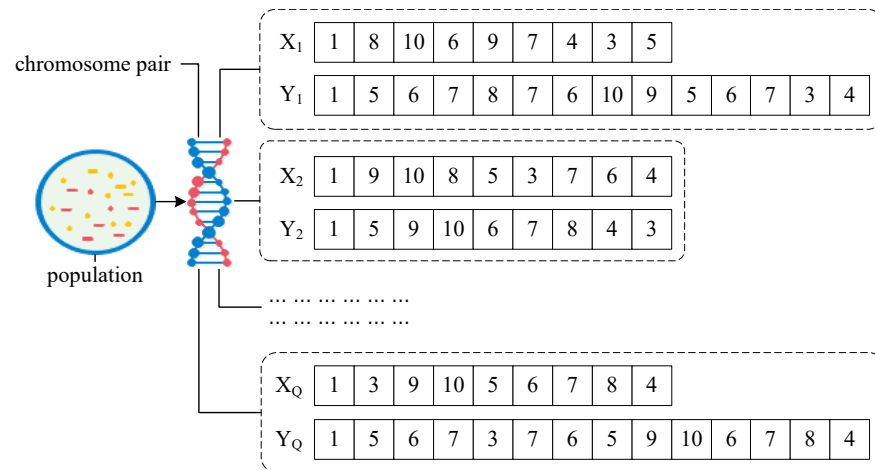


Figure 8. The chromosome pair-based population.

2.2.2. Fitness Calculation Based on Multi-Objective Equalization Criterion

The fitness function is the basis of the genetic algorithm iteration, and is the key factor of generating optimal solution and algorithm convergence. Because the turns and U-turns will produce a deceleration–reacceleration process, and increase the energy consumption of agricultural robot, the main objective of CCPP is to reduce the number of turns and U-turns as much as possible while covering all the free grids. However, in practical farming operation, the number of turns or U-turns was inevitably increased to reduce the repeated work area, or the repeated work area was increased to reduce the number of turns or U-turns. Therefore, to balance the cost of the number of turns, the number of U-turns, and the repeated work area [32], a multi-objective-balance-criterion-based fitness function was proposed in this paper, which was defined as follows

$$f(i) = \frac{1}{w_1(i)\varphi[z_1(i)] + w_2(i)\varphi[z_2(i)] + w_3(i)\varphi[z_3(i)]} \tag{1}$$

where $f(i)$ represents the fitness value of the i -th chromosome; $w_1(i)$, $w_2(i)$ and $w_3(i)$ represent the weight of the repeated work area, the weight of the number of turns and the weight of the number of U-turns, respectively, which were defined in (2) to (7); and $\varphi[z_1(i)]$, $\varphi[z_2(i)]$ and $\varphi[z_3(i)]$ represent the repeated work area, the number of turns and the number of U-turns, which were defined in (11) to (15).

The initial weight of $w_1(i)$, $w_2(i)$, and $w_3(i)$ are set to 0.3, 0.2, and 0.5, then the weight adaptive mechanism was used to balance the three objectives with the following formula,

$$w_1^t(i) = \begin{cases} w_1^{t-1}(i) \times (1 + \frac{\varphi[z_1^t(i)] - \overline{\varphi(Z_1^{t-1})}}{\varphi[z_1^t(i)]}) & , \varphi[z_1^t(i)] > \overline{\varphi(Z_1^{t-1})} \\ w_1^{t-1}(i) & , \varphi[z_1^t(i)] \leq \overline{\varphi(Z_1^{t-1})} \end{cases} \tag{2}$$

$$w_2^t(i) = \begin{cases} w_2^{t-1}(i) \times (1 + \frac{\varphi[z_2^t(i)] - \overline{\varphi(Z_2^{t-1})}}{\varphi[z_2^t(i)]}) & , \varphi[z_2^t(i)] > \overline{\varphi(Z_2^{t-1})} \\ w_2^{t-1}(i) & , \varphi[z_2^t(i)] \leq \overline{\varphi(Z_2^{t-1})} \end{cases} \tag{3}$$

$$w_3^t(i) = \begin{cases} w_3^{t-1}(i) \times (1 + \frac{\varphi[z_3^t(i)] - \overline{\varphi(Z_3^{t-1})}}{\varphi[z_3^t(i)]}) & , \varphi[z_3^t(i)] > \overline{\varphi(Z_3^{t-1})} \\ w_3^{t-1}(i) & , \varphi[z_3^t(i)] \leq \overline{\varphi(Z_3^{t-1})} \end{cases} \tag{4}$$

$$w_1(i) = \frac{w_1^t(i)}{w_1^t(i) + w_2^t(i) + w_3^t(i)} \tag{5}$$

$$w_2(i) = \frac{w_2^t(i)}{w_1^t(i) + w_2^t(i) + w_3^t(i)} \tag{6}$$

$$w_3(i) = \frac{w_3^t(i)}{w_1^t(i) + w_2^t(i) + w_3^t(i)} \tag{7}$$

where $w_1^t(i)$, $w_2^t(i)$ and $w_3^t(i)$ represent the weights of the i -th chromosome in current population; $w_1^{t-1}(i)$, $w_2^{t-1}(i)$ and $w_3^{t-1}(i)$ represent the weight of the i -th chromosome in parent population; $\varphi[z_1^t(i)]$, $\varphi[z_2^t(i)]$ and $\varphi[z_3^t(i)]$ represent the repeated work area, the number of turns and the number of U-turns of the i -th chromosome in current population, respectively; and $\overline{\varphi(Z_1^{t-1})}$, $\overline{\varphi(Z_2^{t-1})}$ and $\overline{\varphi(Z_3^{t-1})}$ represent the average of the repeated work area, the number of turns and the number of U-turns of all chromosomes in parent population, respectively, which were defined in (8) to (10).

$$\overline{\varphi(Z_1^{t-1})} = \sum_i^Q \varphi[z_1^{t-1}(i)] / Q \tag{8}$$

$$\overline{\varphi(Z_2^{t-1})} = \sum_i^Q \varphi[z_2^{t-1}(i)] / Q \tag{9}$$

$$\overline{\varphi(Z_3^{t-1})} = \sum_i^Q \varphi[z_3^{t-1}(i)] / Q \tag{10}$$

The repeated work area $\varphi[z_1(i)]$, the number of turns $\varphi[z_2(i)]$ and the number of U-turns $\varphi[z_3(i)]$ of the i -th chromosome were calculated according to the Y chromosome, which are defined as follows:

$$\varphi[z_1(i)] = ||Y_i|| - ||set(Y_i)|| \tag{11}$$

$$turn(g) = \begin{cases} 1, & |orien(Y_i[g]) - orien([Y_i[g - 1]])| \% 2 = 1 \\ 0, & |orien(Y_i[g]) - orien([Y_i[g - 1]])| \% 2 \neq 1 \end{cases} \tag{12}$$

$$\varphi[z_2(i)] = \sum_{g=1}^{||Y_i||} turn(g) \tag{13}$$

$$uturn(g) = \begin{cases} 1, & |orien(Y_i[g]) - orien([Y_i[g - 1]])| = 2 \\ 0, & |orien(Y_i[g]) - orien([Y_i[g - 1]])| \neq 2 \end{cases} \tag{14}$$

$$\varphi[z_3(i)] = \sum_{g=1}^{||Y_i||} uturn(g) \tag{15}$$

where $||Y_i||$ represents the length of the chromosome Y_i ; $||set(Y_i)||$ represents the length of the chromosome after removing its repeated genes; $\%$ represents the mod operation; $orien(Y_i[g])$ represents the moving direction of the autonomous driving agricultural robot at the grid $Y_i[g]$; and $turn(g)$, $uturn(g)$ represent whether the autonomous driving agricultural robot has the turn and U-turn action at the grid $Y_i[g]$, respectively.

2.2.3. Roulette Selection Operation Based on Elite Strategy

The elitist-strategy-based roulette selection was adopted in this paper to make the optimal k elite chromosomes in the parent population be inherited to the offspring population. In addition, the remaining chromosomes in the parent population are selected by

the roulette algorithm until the desired number of offspring chromosomes are satisfied. Thus, each chromosome has the probability that proportional to its fitness value to enter the offspring generation, and the chromosomes both with low fitness value and high fitness value are selected. This will make the population have the diversity, and make the algorithm avoid falling into a local optimum [33]. The probability $P(i)$ of a chromosome being selected in the population is defined as follows:

$$P(i) = \frac{f(i)}{\sum_{i=1}^Q f(i)} \quad (16)$$

where i represents the i -th chromosome; $f(i)$ represents the fitness value of the i -th chromosome (as shown in (1)); and Q is the total number of chromosome in the population.

2.2.4. Crossover Operation Based on Order-Preserving Method

Crossover is one of the important steps in the evolution of genetic algorithm, which is analogous to reproduction and biological crossover. In crossover operation, more than one parent is selected with a high probability and one or more off-springs are produced using the genetic material of the parents, which will enhance the algorithm's optimization ability. The order-preserving crossover method was used in this paper, which was detailed as follows. Firstly, two chromosomes, A and B, were randomly selected for crossover in the parent population. Then a crossover point of chromosome A was randomly determined, and the genes behind this point in chromosome A were deleted. Next the genes at the front of the crossover point in chromosome A were deleted from chromosome B. Finally, the remaining genes in chromosome B were added behind the crossover point of chromosome A, and a new chromosome C will be obtained. The crossover probability is generally between 0.5 and 1. The crossover not only ensures that the off-spring chromosome contains all the free grids, but also has the characteristics of the parent chromosome.

For example, the order-preserving crossover operation are shown in Figure 9. Firstly, as shown in Figure 9a, the crossover point was randomly determined, i.e., gene 6 in chromosome 1 and gene 8 in chromosome 2. Then, as shown in Figure 9b, gene 1, 8, and 10 (appeared before the crossover point in chromosome 1) were deleted in chromosome 2, and the genes (i.e., gene 9, 7, 4, 3, and 5) behind the crossover point in chromosome 1 were deleted. Finally, as shown in Figure 9c, the remaining gene sequence 3-7-5-9-4 was added in order behind the crossover point of chromosome 1, and the off-spring chromosome 1-8-10-6-9-7-4-3-5 can be obtained. Similarly, the off-spring chromosome generated by the order-preserving crossover operation also should be adjusted by the method in Section 2.2.1 to calculate its fitness value.

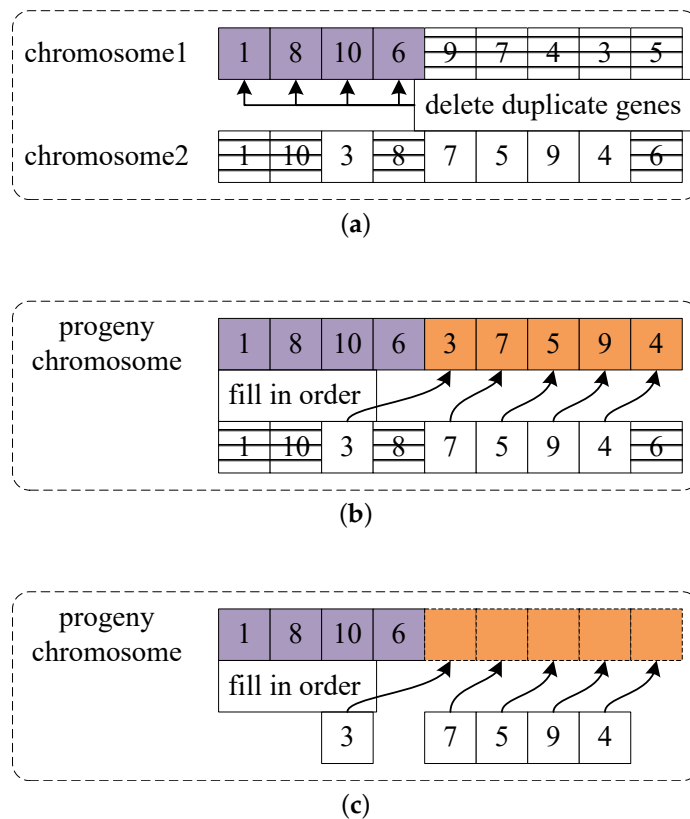


Figure 9. The order-preserving crossover. (a) Determine the crossover point. (b) Delete duplicate gene. (c) Fill the remaining genes in order.

2.2.5. Mutation Operation Based on Multi-Points Method

Mutation is one of the important steps in the evolution of genetic algorithm. Mutation can be defined as a small random tweak in the chromosome to obtain a new solution, which can maintain and introduce diversity in the genetic population. It is usually applied with a low probability since the GA will become reduced to a random search if the probability is very high. Mutation is essential to the convergence of the genetic algorithm. A novel mutation operation, namely multi-points mutation, was proposed in this paper to improve the ability to search for the optimal solution, which is described as follows. Firstly, the number (m) of gene pairs for mutation was randomly determined, and the gene positions of the m pairs for mutation were also randomly determined. Then, the two genes in each pair of mutation points were exchanged, and, finally, a new chromosome can be obtained. The mutation probability is generally between 0.001 and 0.1. The multi-points mutation can significantly destroy the gene sequence of the parent while ensures that the off-spring chromosome contains all the free grids, which helps the algorithm avoid to fall in local optimum.

For example, the multi-points mutation operation was shown in Figure 10. Firstly, two mutation points were randomly identified, e.g., gene 6 and gene 7 in Figure 10a. Then keeping the gene 1 unchanged, the chromosome segments before gene 6 and after gene 7 were interchanged, as shown in Figure 10b. Finally, the progeny chromosome 1-4-3-5-6-7-8-10 after mutation was obtained. Similarly, the progeny chromosome generated by the multi-points mutation operation also should be adjusted by the method in Section 2.2.1 to calculate its fitness value.

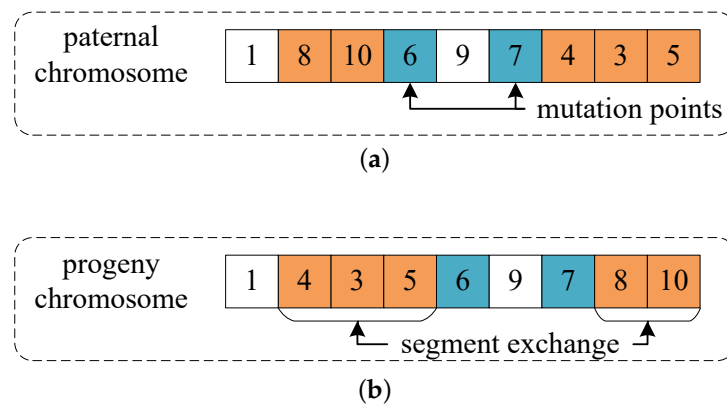


Figure 10. The multi-points mutation operation. (a) Determine the mutation points (b) Swap segment of genes.

2.3. Outputting the Optimal Complete Coverage Path

Genetic algorithm usually has two conditions of termination, (1) setting the maximum number of generations, and (2) the fitness tends to stable. The former was that when the maximum number of iterations was reached, the algorithm was terminated and output the optimal solution. The latter was that when the fitness value of the optimal solution was less than the pre-set threshold δ or the fitness value was unchanged for many iterations (e.g., M times, which also was preset), the algorithm can be terminated and output the optimal solution. Both conditions were adopted in this paper, the maximum number of iterations was set, and if the condition (2) was satisfied, the algorithm can be terminated early; otherwise, the algorithm will be terminated until the maximum number of iterations was reached.

When the algorithm was terminated, the OCCP, i.e., the adjusted chromosome Y in the chromosome pair can be acquired. For example, if the optimal solution was the optimal adjusted chromosome *chromosome** shown in Figure 11a, its corresponding OCCP was shown in Figure 11b.

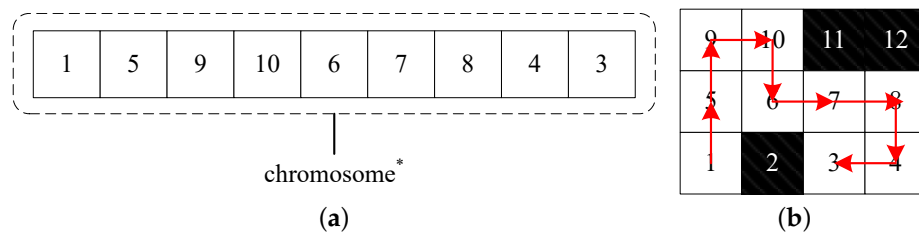


Figure 11. The OCCP. (a) The Y chromosome in optimal pair (b) OCCP.

3. Results and Discussion

Heuristic algorithm is a basic method to solve optimization problems [34], four fields with different shapes were used for evaluating the performance of the proposed improved-genetic-algorithm-based CCPP method, such as the algorithm convergence, the feasibility and optimality of the planned path. All the test experiments were performed on the transplanter (as shown in Figure 12a, 2ZB-2B, DingDuo robot Co., Ltd., Baoji, China) with automatic navigation ability. The transplanter has the shape of 3050 × 2000 × 1750 (mm) (length × width × height). The automatic navigation system was the Beidou automatic navigation and driving system (AF301, Lianshi Navigation Technology Co., Ltd., Shanghai, China), which includes the double antenna satellite receiver (R71, Lianshi Navigation Technology Co., Ltd., Shanghai, China), the steering controller (EMS2, Lianshi Navigation Technology Co., Ltd., Shanghai, China), the angle sensor (Vert-X 26, Contelec AG, Bienne, Switzerland), the IMU (S31, Lianshi Navigation Technology Co., Ltd., Shanghai, China),

and the vehicle-mounted information terminal (T100, Lianshi Navigation Technology Co., Ltd., Shanghai, China). The proposed CCPP method was deployed on the microprocessor (Jetson Nano, Nvidia Corp., Santa Clara), and the microprocessor connect with the vehicle-mounted information terminal through the RS232 interface. The connection between modules is shown in Figure 12b.

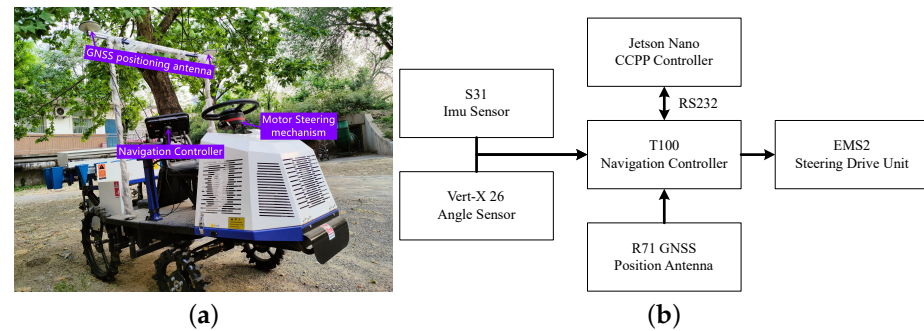


Figure 12. Automatic guided transplanter. (a) Transplanter. (b) Hardware structure.

3.1. Experiments Settings

Environment map selection: One rectangular field A without obstacles (as shown in Figure 13a), one rectangular field B with obstacles (as shown in Figure 13b), one polygonal field C without obstacles (as shown in Figure 13c), and one polygonal field D with obstacles (as shown in Figure 13d) were selected for testing the proposed CCPP method. The minimum bounding rectangles of the selected four fields have the same shape, i.e., 40 m long and 24 m wide. Then, the four fields were encoded as the grid maps (as shown in Figure 14 using the method in Section 2.1. The grid size was set to 2 m \times 2 m according to the working width of the transplanter in Figure 12.

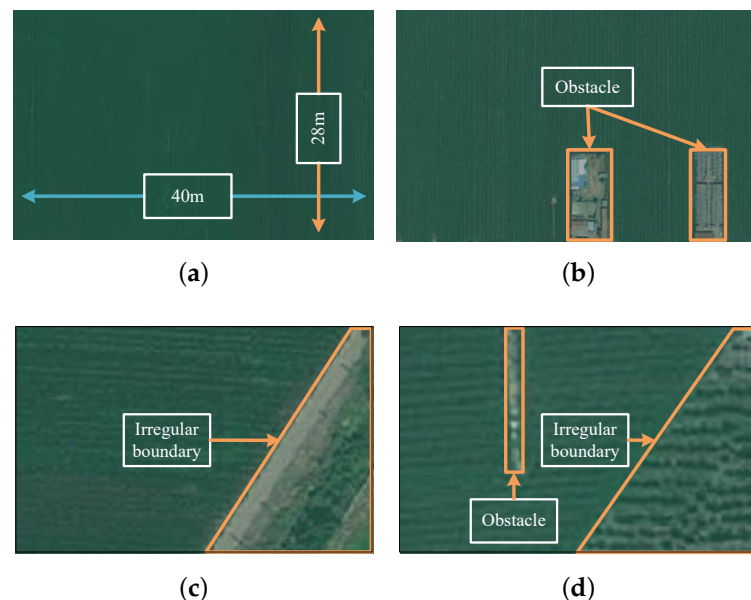


Figure 13. Multi-topographic field map. (a) Barrier-free rectangular field. (b) Rectangular field with obstacles. (c) Barrier-free irregularity field. (d) Irregularity field with obstacles.

In this paper, the selected four multi-topographic fields are processed through the environment map modeling based on the grid method, and the fields are rasterized according to the automatic driving agricultural robot with the work breadth of 2 m. Firstly, the fields are divided into grids with equal areas, with a grid area of 4 m². Secondly, the boundary

area and obstacle area are to be dilated into a regular-shaped map. Furthermore, finally, encoding the grid map to obtain four grid maps as shown in Figure 14.

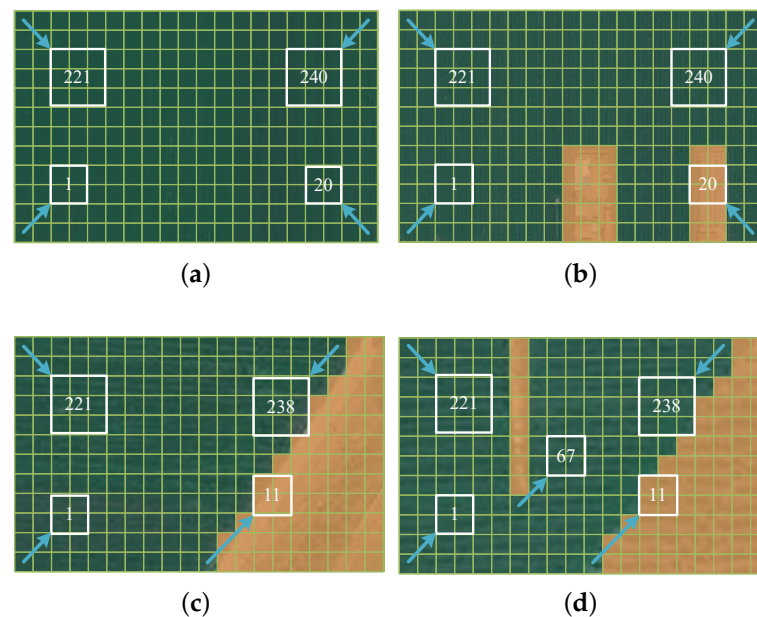


Figure 14. Coded multi-topographic field map. (a) Coded barrier-free rectangular field. (b) Coded rectangular field with obstacles. (c) Coded barrier-free irregularity field. (d) Coded irregularity field with obstacles.

Parameters setting: The parameters of the proposed improved genetic algorithm were set to the same for all the selected testing fields. The number Q of the chromosome pairs in initial population was 200, the crossover probability of chromosomes was 0.5, the mutation probability of chromosomes was 0.01, and the number of iterations T was 5000. For the initial weights (i.e., $w_1(i)$, $w_2(i)$ and $w_3(i)$) in (1) of the repeated work area, the number of turns and the number of U-turns for fitness calculation were 0.3, 0.5, and 0.2, respectively. The elitist preservation strategy was adopted to ensure that the optimal chromosomes of each generation are inherited to the next generation, and the k in roulette selection was set to 1. The number of stable iterations M was set to 500; thus, when the fitness value was not changed for 500 consecutive times or the difference from the target value is less than 0.001, the algorithm will terminate in advance. The code of the algorithm proposed in this paper is written in C++ language, and run the program on a computer with Windows 11 operating system, Intel(R) Core(TM) i7-11800H processor, and 16GB memory. The average time of running 1000 iterations on a map with grid number 12×20 is 215 s. The running time will change with the number of grids and the number of iterations. When the number of grids and the number of iterations increase, the running time of the algorithm will increase accordingly.

3.2. Convergence Test of the Algorithm

To test the proposed multi-points mutation effect on the algorithm convergence and the global optimization-seeking ability, the single-point mutation was selected for comparison. The parameters for multi-points and single-point mutation were set to the same as in Section 3.1, and the fitness values of the 1000 iterations were counted, as shown in Figure 15. The results shown in Figure 15 showed that the proposed multi-points mutation has a higher evolutionary efficiency than the single-point mutation. The fitness values of the 1000th iteration on the field A, B, C, and D calculated by the multi-points-mutation-based algorithm were 0.22727, 0.18519, 0.26316, and 0.11364, respectively, exceeding the fitness values calculated by the single-point-mutation-based algorithm, i.e., 0.16393, 0.12048,

0.15625, and 0.09804. This indicated that the global optimization-seeking ability of the multi-points mutation was increased comparing with the single-point mutation.

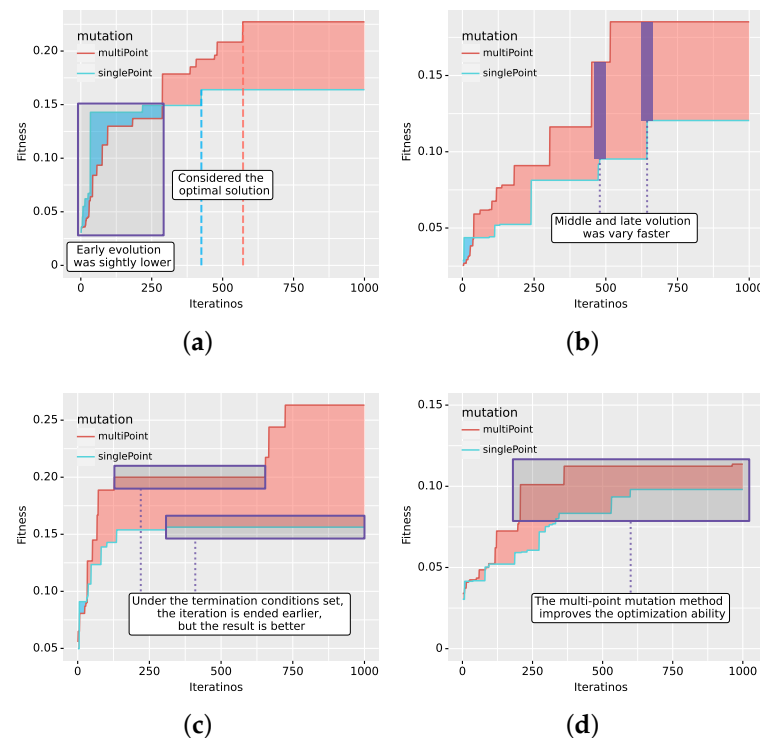


Figure 15. Comparison of multi-point and single-point mutation. (a) The algorithm convergence on field A. (b) The algorithm convergence on field B. (c) The algorithm convergence on field C. (d) The algorithm convergence on field D.

As shown in Figure 15, the evolution speed of the improved genetic algorithm proposed in this paper was faster than that of the traditional genetic algorithm. This is because the order-preserving crossover method and multi-point mutation method can destroy the gene rank of the parent chromosome to the greatest extent, which can accelerate the algorithm to overstep the local extremum. As shown in Figure 15a,b, in the regular-shaped field experiment, the multi-point mutation method has a stronger search ability than the single-point mutation method in both field A and B, especially in the field with obstacles (i.e., Field B). As shown in Figure 15c, in the experiment of irregular-shaped field C, although the multi-point mutation method stopped earlier than the single-point mutation method, it has a higher fitness value. As shown in Figure 15c,d, the multi-point mutation method improves the optimization ability of the algorithm at the later stage, and can find a better solution than the single point mutation. In addition, these are indicated that the algorithm has a strong adaptability in both regular-shaped and irregular-shaped fields.

3.3. Path Feasibility Test of the Algorithm

For testing the feasibility of the planned path, the traditional genetic algorithm with one chromosome-based CCP method was used for comparison. The paths (as shown in Figure 16) planned by the traditional genetic algorithm were disorganized for all testing fields. This is because the adjacent genes in the chromosome of the traditional genetic algorithm do not satisfy the 4-neighbor relationship, resulting in the excessive randomness of the planned path that the transplanting robot cannot follow. However, the proposed chromosome-pair-based genetic algorithm can plan the feasible path (as shown in Figure 17, since all adjacent genes in chromosome Y satisfy the 4-neighbor relationship with each other. The chromosome Y represents a complete coverage path that the transplanting robot can follow.

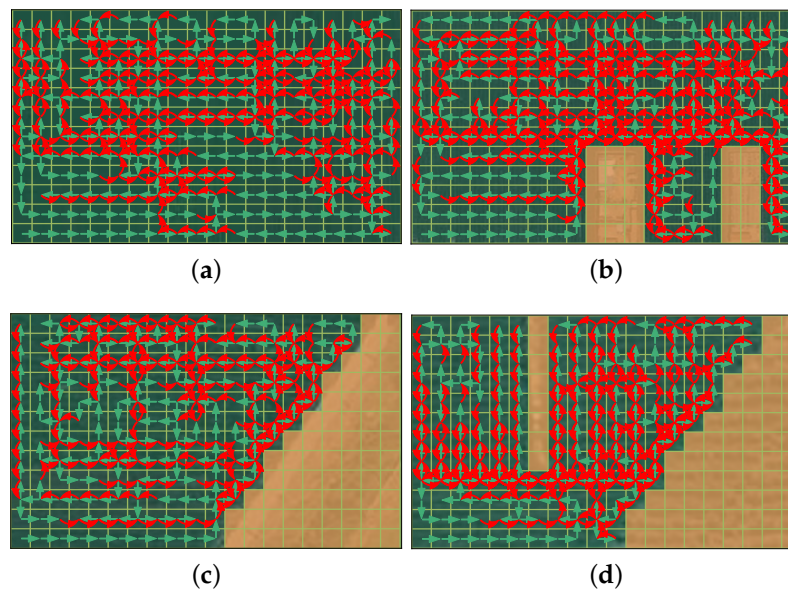


Figure 16. Multi-topographic field path planning based on single chromosome. (a) CCP of A based on single chromosome. (b) CCP of B based on single chromosome. (c) CCP of C based on single chromosome. (d) CCP of D based on single chromosome.

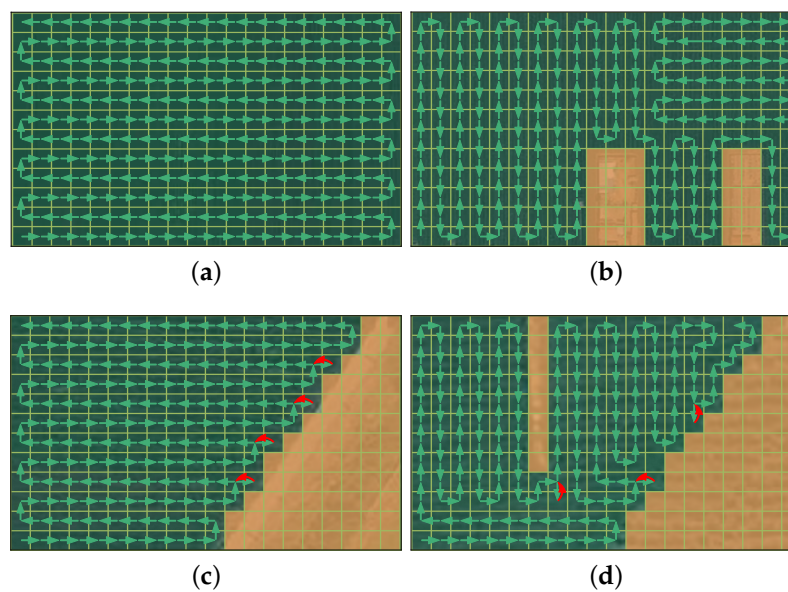


Figure 17. Multi-topographic field path planning based on chromosome pairs. (a) CCP of field A based on chromosome pairs. (b) CCP of field B based on chromosome pairs. (c) CCP of field C based on chromosome pairs. (d) CCP of field D based on chromosome pairs.

3.4. Path Optimality Test of the Algorithm

To test the optimality of the path planned by the proposed improved-genetic-algorithm-based CCPP method, the boustrophedon-based complete coverage method was used for comparison, and its planned path was shown in Figure 18. Its basic idea was to use the “bow” type search method to cover the field, i.e., the transplanting robot works back and forth along the longest edge of the field. Furthermore, when encountering an obstacle, it moves a grid up to cross the obstacle, then returns to the previous working path. If the field boundary was reached, it moves back. The above steps were repeated until all the field were covered.

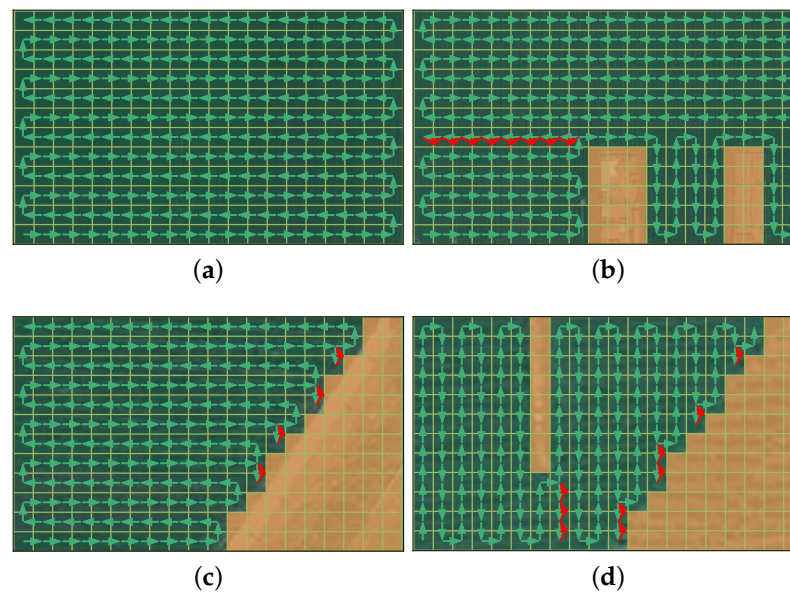


Figure 18. Multi-topographic field path planning based on boustrophedon method. (a) CCP of field A based on boustrophedon. (b) CCP of field B based on boustrophedon. (c) CCP of field C based on boustrophedon. (d) CCP of field D based on boustrophedon.

3.5. Experimental Results in Real Transplanting Robot

As shown in Figure 18, it can be seen that the complete coverage path generated by the boustrophedon algorithm is more regular, showing a “bow” type operation pattern; however, there are more repetitive operation area and the number of U-turns. The complete coverage path generated by the proposed method (Figure 17) has less repetitive operation area and number of U-turns. We use the transplanting robot shown in Figure 12 to test the complete coverage operation in four multi-terrain fields using the boustrophedon method and the method in this paper, and the final energy consumption in the field is calculated by calculating the percentage drop of battery voltage. Field A is a barrier-free rectangular area, and the planning paths of boustrophedon method and this paper are the same, and there is no significant change in each index. Field D is an barrier irregular-shaped area, the area of repeated operation and the number of U-turns decreased significantly. In addition, as shown in Table 2, the comprehensive energy consumptions of the boustrophedon method in four multi-topographic fields are 29%, 71%, 56%, and 85%, respectively. Furthermore, the comprehensive energy consumptions of the method in this paper are 29%, 66%, 51%, and 72%, respectively. This is because the method in this paper focuses on the complex farming environment, such as irregular-shaped boundary and obstacle in field, which is more suitable for field B, field C, and field D. Therefore, the CCPP method in this paper is more capable in complex fields.

Complete coverage path planning focuses on saving comprehensive energy consumption [35], it can be seen from the comparison between the boustrophedon method and improved-genetic-algorithm-based method in Table 3 and Figure 19. In four multi-topographic fields, all indicators are reduced except for a slight increase in the number of turns, which is due to the equilibrium adaptation fitness with multiple indicators. There will not be significant increases in the number of turns while reducing the area of repeated area and the number of U-turns. The advantage of the CCPP based on in this paper in field D is the most obvious, followed by field B and field C. In addition, with an average increase of 13.76% in the number of turns, the repetitive operation area, the number of turnarounds and the comprehensive energy consumption are reduced by 38.54%, 35.00%, and 7.82% on average. Although the CCPP method in this paper may increase the number of turns, the repeated operation area and the number of U-turns are decreased, and the comprehensive energy consumption is significantly reduced.

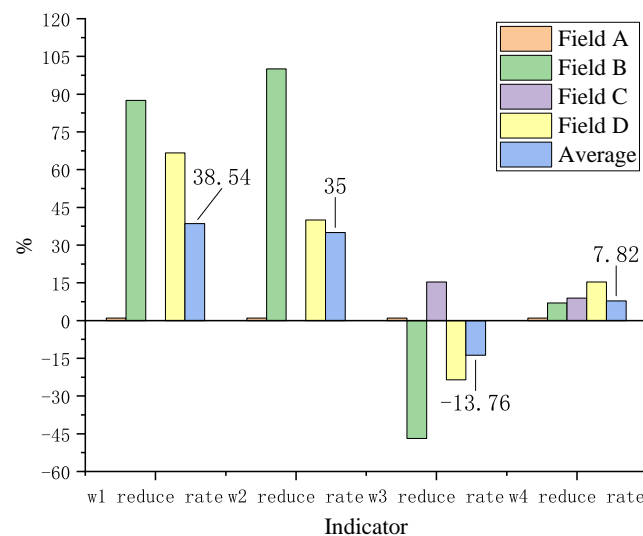
Table 2. Path planning data of multi-topographic field with complete coverage.

| Indicator | Method | Field A | Field B | Field C | Field D | Average |
|-------------------|---------------|---------|---------|---------|---------|---------|
| w1/m ² | boustrophedon | 0 | 32 | 16 | 36 | 21.00 |
| | our method | 0 | 4 | 16 | 12 | 8.00 |
| w2/time | boustrophedon | 22 | 32 | 26 | 34 | 28.50 |
| | our method | 22 | 47 | 22 | 42 | 33.25 |
| w3/time | boustrophedon | 0 | 1 | 4 | 5 | 2.50 |
| | our method | 0 | 0 | 4 | 3 | 1.75 |
| w4 | boustrophedon | 29% | 71% | 56% | 85% | 60.25% |
| | our method | 29% | 66% | 51% | 72% | 54.50% |

Note: w1, w2, w3, and w4 represents the repeated area, the turns number, the U-turns number and the consumed battery voltage, respectively.

Table 3. Comparison between boustrophedon method and provided method in this paper.

| Indicator | Field A | Field B | Field C | Field D | Average |
|--------------------------|---------|---------|---------|---------|---------|
| w1 reduce/m ² | 0 | 28 | 0 | 24 | 13.00 |
| w2 reduce/time | 0 | −15 | 4 | −8 | −4.75 |
| w3 reduce/time | 0 | 1 | 0 | 2 | 0.75 |
| w4 reduce | 0% | 5% | 5% | 13% | 5.75% |

**Figure 19.** Comparison percentage chart of each indicator.

According to the above analysis, compared with the boustrophedon method, the proposed method in this paper can minimize the repeated operation area and reduce the number of U-turns, which can help improve the operation efficiency of transplanting robot and reduce the operation energy consumption cost. It is more capable of planning a complete coverage path for the real operation of self-driving transplanting robots, which is more adaptable to the environment and has practical application value.

4. Conclusions

In this paper, the improved-genetic-algorithm is proposed to plan the complete coverage of the field of autonomous driving agricultural robot. Compared with the standard genetic algorithm, it has the following advantages. A chromosome adjustment method suitable for CCPP is designed to generate chromosome pairs, in which the number of chromosome genes before adjustment is the same, which is used for evolution operations, such as crossover and mutation. The number of adjusted chromosome genes is not necessarily the same, but each genes and their neighboring genes are consecutively adjacent in the

grid-map, representing a feasible complete coverage path. Furthermore, we designed a multi-point mutation method, compared with single-point mutation, it can destroy the locus of the parent chromosome and has better global optimization ability. In order to verify the effectiveness of the algorithm proposed, the method in this paper and the boustrophedon method are used for CCP for the four different types of actual fields. The complete coverage of the actual operation of agricultural robot reduces unnecessary mileage and improves operation efficiency. Next, this paper considers path planning for large-area fields to propose a new method that can handle large-scale grids. At the same time, the popular deep learning technology is used to improve the accuracy and efficiency of the algorithm, and multiple plots are studied to further improve the practicability of field path planning. The complete coverage path planning method based on grid method and improved genetic algorithm studied in this paper is mainly aimed at the field of self-driving agricultural robots. Of course, it can also be applied to broader scenarios, such as cleaning robots, demining robots, and plant protection drones and other fields.

Author Contributions: Conceptualization, X.W. and J.B.; methodology, X.W., J.B. and F.H.; software, X.W. and X.L.; validation, X.W., J.B. and X.L.; formal analysis, G.C.; investigation, Y.T.; resources, F.H.; data curation, F.H.; writing—original draft preparation, X.W. and J.B.; writing—review and editing, X.W., J.B. and Y.T.; visualization, X.L.; supervision, G.C.; project administration, F.H. All authors have read and agreed to the published version of the manuscript.

Funding: This research was funded by the Young Scientists Fund of the National Natural Science Foundation of China (42201458), the Major Science and Technology Innovation Project of Shan-dong Province (2019JZZY020603, the Shandong Province Natural Science Youth Foundation of China (ZR2021QF131), and the Qilu University of Technology (Shandong Academy of Sciences) Science-Education-Industry integration pilot project plan (2022PT097).

Data Availability Statement: Not applicable.

Acknowledgments: The authors wish to express sincere gratitude to Baoji DingDuo Machinery Co., Ltd. for the transplanter and Shanghai Lianshi Navigation Technology Co., Ltd. for providing the assisted driving system and its technical support.

Conflicts of Interest: The authors declare no conflict of interest.

References

1. Langer, T.H. Model-in-the-Loop Tuning of Hitch Control Systems of Agricultural Tractors. In Proceedings of the 75th VDI Internationale Tagung Landtechnik (Agricultural Engineering), Hanover, Germany, 10–11 November 2017.
2. Liang, X.; Liu, C.; Zeng, Z. Multi-Domain Informative Coverage Path Planning for a Hybrid Aerial Underwater Vehicle in Dynamic Environments. *Machines* **2021**, *9*, 278. [[CrossRef](#)]
3. Han, G.; Zhou, Z.; Zhang, T.; Wang, H.; Liu, L.; Peng, Y.; Guizani, M. Ant-colony-based complete-coverage path-planning algorithm for underwater gliders in ocean areas with thermoclines. *IEEE Trans. Veh. Technol.* **2020**, *69*, 8959–8971. [[CrossRef](#)]
4. Luo, B.; Huang, Y.; Deng, F.; Li, W.; Yan, Y. Complete Coverage Path Planning for Intelligent Sweeping Robot. In Proceedings of the 2021 IEEE Asia-Pacific Conference on Image Processing, Electronics and Computers (IPEC), Dalian, China, 14–16 April 2021; pp. 316–321.
5. Li, C.h.; Fang, C.; Wang, F.y.; Xia, B.; Song, Y. Complete coverage path planning for an arnold system based mobile robot to perform specific types of missions. *Front. Inf. Technol. Electron. Eng.* **2019**, *20*, 1530–1542. [[CrossRef](#)]
6. Jin, J.; Tang, L. Optimal coverage path planning for arable farming on 2D surfaces. *Trans. ASABE* **2010**, *53*, 283–295. [[CrossRef](#)]
7. Jin, J.; Tang, L. Coverage path planning on three-dimensional terrain for arable farming. *J. Field Robot.* **2011**, *28*, 424–440. [[CrossRef](#)]
8. Yin, X.; Wang, Y.; Chen, Y.; Jin, C.; Du, J. Development of autonomous navigation controller for agricultural vehicles. *Int. J. Agric. Biol. Eng.* **2020**, *13*, 70–76. [[CrossRef](#)]
9. Adegbola, Y.U.; Fisher, P.R.; Hodges, A.W. Economic evaluation of transplant robots for plant cuttings. *Sci. Hortic.* **2019**, *246*, 237–243. [[CrossRef](#)]
10. Edwards, G.T.; Hinge, J.; Skou-Nielsen, N.; Villa-Henriksen, A.; Sørensen, C.A.G.; Green, O. Route planning evaluation of a prototype optimised infield route planner for neutral material flow agricultural operations. *Biosyst. Eng.* **2017**, *153*, 149–157. [[CrossRef](#)]
11. Seyyedhasani, H.; Dvorak, J.S. Reducing field work time using fleet routing optimization. *Biosyst. Eng.* **2018**, *169*, 1–10. [[CrossRef](#)]

12. Zafar, M.N.; Mohanta, J. Methodology for path planning and optimization of mobile robots: A review. *Procedia Comput. Sci.* **2018**, *133*, 141–152. [[CrossRef](#)]
13. Lee, T.K.; Baek, S.H.; Choi, Y.H.; Oh, S.Y. Smooth coverage path planning and control of mobile robots based on high-resolution grid map representation. *Robot. Auton. Syst.* **2011**, *59*, 801–812. [[CrossRef](#)]
14. Valente, J.; Del Cerro, J.; Barrientos, A.; Sanz, D. Aerial coverage optimization in precision agriculture management: A musical harmony inspired approach. *Comput. Electron. Agric.* **2013**, *99*, 153–159. [[CrossRef](#)]
15. Ammar, A.; Bennaceur, H.; Châari, I.; Koubâa, A.; Alajlan, M. Relaxed Dijkstra and A* with linear complexity for robot path planning problems in large-scale grid environments. *Soft Comput.* **2016**, *20*, 4149–4171. [[CrossRef](#)]
16. Choset, H.; Pignon, P. Coverage path planning: The boustrophedon cellular decomposition. In *Field and Service Robotics*; Springer: Berlin/Heidelberg, Germany, 1998; pp. 203–209.
17. Huang, W.H. Optimal line-sweep-based decompositions for coverage algorithms. In Proceedings of the Proceedings 2001 ICRA. IEEE International Conference on Robotics and Automation (Cat. No. 01CH37164), Seoul, Republic of Korea, 21–26 May 2001; Volume 1, pp. 27–32.
18. Yang, S.X.; Luo, C. A neural network approach to complete coverage path planning. *IEEE Trans. Syst. Man Cybern. Part (Cybern.)* **2004**, *34*, 718–724. [[CrossRef](#)]
19. Luo, C.; Yang, S.X. A bioinspired neural network for real-time concurrent map building and complete coverage robot navigation in unknown environments. *IEEE Trans. Neural Netw.* **2008**, *19*, 1279–1298. [[CrossRef](#)]
20. Xu, P.F.; Ding, Y.X.; Luo, J.C. Complete Coverage Path Planning of an Unmanned Surface Vehicle Based on a Complete Coverage Neural Network Algorithm. *J. Mar. Sci. Eng.* **2021**, *9*, 1163. [[CrossRef](#)]
21. Mazzia, V.; Salvetti, F.; Aghi, D.; Chiaberge, M. Deepway: a deep learning waypoint estimator for global path generation. *Comput. Electron. Agric.* **2021**, *184*, 106091. [[CrossRef](#)]
22. Liang, X.D.; Li, L.Y.; Wu, J.G.; Chen, H.N. Mobile robot path planning based on adaptive bacterial foraging algorithm. *J. Cent. South Univ.* **2013**, *20*, 3391–3400. [[CrossRef](#)]
23. Conesa-Muñoz, J.; Pajares, G.; Ribeiro, A. Mix-opt: A new route operator for optimal coverage path planning for a fleet in an agricultural environment. *Expert Syst. Appl.* **2016**, *54*, 364–378. [[CrossRef](#)]
24. Le, A.V.; Arunmozhi, M.; Veerajagadheswar, P.; Ku, P.C.; Minh, T.H.Q.; Sivanantham, V.; Mohan, R.E. Complete path planning for a tetris-inspired self-reconfigurable robot by the genetic algorithm of the traveling salesman problem. *Electronics* **2018**, *7*, 344. [[CrossRef](#)]
25. Fountas, N.A.; Benhadj-Djalili, R.; Stergiou, C.I.; Vaxevanidis, N.M. An integrated framework for optimizing sculptured surface CNC tool paths based on direct software object evaluation and viral intelligence. *J. Intell. Manuf.* **2019**, *30*, 1581–1599. [[CrossRef](#)]
26. Mahmud, M.S.A.; Abidin, M.S.Z.; Mohamed, Z.; Abd Rahman, M.K.I.; Iida, M. Multi-objective path planner for an agricultural mobile robot in a virtual greenhouse environment. *Comput. Electron. Agric.* **2019**, *157*, 488–499. [[CrossRef](#)]
27. Le, A.V.; Nhan, N.H.K.; Mohan, R.E. Evolutionary algorithm-based complete coverage path planning for tetramond tiling robots. *Sensors* **2020**, *20*, 445. [[CrossRef](#)]
28. Jeon, C.W.; Kim, H.J.; Yun, C.; Gang, M.; Han, X. An entry-exit path planner for an autonomous tractor in a paddy field. *Comput. Electron. Agric.* **2021**, *191*, 106548. [[CrossRef](#)]
29. Zeng, C.; Zhang, Q.; Wei, X.P. Global Path Planning for Full-Area Coverage Robotic Systems by Employing an Active Genetic Algorithm. In *Advanced Materials Research*; Trans Tech Publications Ltd.: Bâch, Switzerland, 2011; Volume 328, pp. 1881–1886.
30. Horn, J.; Nafpliotis, N.; Goldberg, D.E. A niched Pareto genetic algorithm for multiobjective optimization. In Proceedings of the First IEEE Conference on Evolutionary Computation. IEEE World Congress on Computational Intelligence, Orlando, FL, USA, 27–29 June 1994; pp. 82–87.
31. Hougardy, S. The Floyd–Warshall algorithm on graphs with negative cycles. *Inf. Process. Lett.* **2010**, *110*, 279–281. [[CrossRef](#)]
32. Osanlou, K.; Guettier, C.; Bursuc, A.; Cazenave, T.; Jacopin, E. Learning-based preference prediction for constrained multi-criteria path-planning. *arXiv* **2021**, arXiv:2108.01080.
33. Razali, N.M.; Geraghty, J. Genetic algorithm performance with different selection strategies in solving TSP. In Proceedings of the World Congress on Engineering, Hong Kong, China, 6–8 July 2011; International Association of Engineers: Hong Kong, China, 2011; Volume 2, pp. 1–6.
34. Dai, J.; Qiu, J.; Yu, H.; Zhang, C.; Wu, Z.; Gao, Q. Robot Static Path Planning Method Based on Deterministic Annealing. *Machines* **2022**, *10*, 600. [[CrossRef](#)]
35. Qin, Y.; Fu, L.; He, D.; Liu, Z. Improved Optimization Strategy Based on Region Division for Collaborative Multi-Agent Coverage Path Planning. *Sensors* **2023**, *23*, 3596. [[CrossRef](#)]

Disclaimer/Publisher’s Note: The statements, opinions and data contained in all publications are solely those of the individual author(s) and contributor(s) and not of MDPI and/or the editor(s). MDPI and/or the editor(s) disclaim responsibility for any injury to people or property resulting from any ideas, methods, instructions or products referred to in the content.